

Structural Analysis of Disk Galaxies of the NGC 524 Group

M. A. Il'ina and O. K. Sil'chenko*

Sternberg Astronomical Institute, Lomonosov Moscow State University, Moscow, Russia

Received February 24, 2012; in final form, March 2, 2012

Abstract—Members of the NGC 524 group of galaxies are studied using data obtained on the 6-m telescope of the Special Astrophysical Observatory of the Russian Academy of Sciences, with the SCORPIO reducer in an imaging mode. Surface photometry has been carried out and parameters of the large-scale structural components—disks and bulges—have been determined for the six largest galaxies of the group. A lowered percentage of bars and enhanced percentage of ring structures were found. The integrated $B-V$ colors of a hundred of dwarf galaxies in the vicinity (within 30 kpc) of the six largest galaxies of the group have been measured. A considerable number of blue irregular galaxies with ongoing star formation is present among nearby dwarf satellites of lenticular galaxies of the group. The luminosity function for dwarf members of the group suggests that the total mass of the group is not very high, and that the X-ray emitting gas observed in the direction of NGC 524 does not belong to the group halo.

DOI: 10.1134/S1063772912080045

1. INTRODUCTION

Groups of galaxies are convenient objects for studies of interactions and the evolution of galaxies subject to external factors. The probability of the development of gravitational tidal effects during close passages is highest in groups, due to both the presence of close neighbors and the low relative velocities of passages between group galaxies. Groups, especially massive ones, often contain hot (X-ray), diffuse gas, which interacts with the cool gas of the galaxies themselves; this interaction is considered to be one reason for the dearth of cool gas in disk galaxies that are members of groups.

So-called “external secular evolution” (see the review [1]) is a slow change of the global properties of galaxies subject to external factors. Secular evolution accumulates strictly determined imprints on the large-scale structures of galaxies: the structure of their disks becomes more complex, and additional structural components, such as bars, rings, and circumnuclear disks, arise in central regions. The dynamical properties of the stellar subsystems also change: the stellar disk becomes thicker during the evolution, the vertical velocity dispersion of its stars increases, etc. Therefore, the large-scale structures of galaxies can be studied most effectively using a multi-faceted approach, beginning with the surface photometry, and then more clearly elucidating the nature of the structural components using spectral observations and kinematic measurements. In the current paper, which is the first of our studies devoted to

the nearby, rich NGC 524 group, we present surface photometry for a number of bright member galaxies. These photometric data were obtained at the 6-m telescope of the Special Astrophysical Observatory (SAO) of the Russian Academy of Sciences.

The NGC 524 group is well known, and has been studied for a long time, due to its location in a relatively sparsely populated place in the Northern sky. It was first cataloged by Geller and Huchra [2], when only eight galaxies were identified as members. Later, Vennik [3] found 18 bright members and 13 dwarf members based on an analysis of Palomar Atlas images using the force hierarchy clustering method, and Brough et al. [4] identified 16 members using the “friends-of-friends” algorithm. The NGC 524 group also has 16 bright members in the last catalog of nearby galaxy groups of Makarov and Karachentsev [5]. Most of the bright members of the group are classified as lenticular galaxies; the fraction of early-type galaxies is estimated to be 0.56 ± 0.15 over the entire luminosity range [4]. The velocity dispersion of the group galaxies is about 180–190 km/s [3, 4], making the group fairly massive ($1.7 \times 10^{13} M_{\odot}$) and compact ($r_{500} = 0.26$ Mpc [4], $r_{500} = 0.42$ Mpc [6]). The ROSAT satellite mapped the X-ray emitting gas in the NGC 524 group, but since the radius of the detected X-ray spot is less than 60 kpc, the hot X-ray gas is considered to belong to the central galaxy of the group and not the group itself [7].

c We have studied the structure of the six brightest galaxies of the group—four lenticular and two early-type spiral galaxies—in detail. Their global char-

*E-mail: sil@sai.msu.su

Table 1. Global parameters of the galaxies

Parameter	NGC 502	NGC 509	NGC 516	NGC 518	NGC 524	NGC 532
Morphological type (NED ¹)	SA 0 ⁰ (r)	S0?	S0	Sa:	SA 0+(rs)	Sab?
R_{25} , arcsec (RC3 ²)	34	43	39	52	85	75
R_{25} , kpc (RC3 + NED)	4.0	5.0	4.5	6.0	9.9	8.7
B_T^0 (RC3)	13.57	14.20	13.97	13.56	11.17	12.91
M_B (RC3 + NED)	-18.3	-17.7	-17.9	-18.3	-20.7	-19.0
$B-V$ (RC3)	0.91	—	—	—	1.00	0.80
V_r , km/s (NED)	2489	2274	2451	2725	2379	2361
Distance from the group center, kpc ([9], NED)	282	151	68	101	0	126
Distance to the group, Mpc [10]	24					

¹ NASA/IPAC Extragalactic Database.

² Third Reference Catalogue of Bright Galaxies [8].

acteristics collected from extragalactic databases are given in Table 1.

2. OBSERVATIONS

The photometric observations analyzed here were obtained at the prime focus of the 6-m telescope of the SAO with the SCORPIO reducer [11] in a direct-imaging mode. The detector was an 2048 × 2048 pixel EEV 42–40 CCD array (with a pixel size of 13.5 μm); the readout was performed in a double-pixel mode, yielding a sampling of 0.35″–0.36″ per pixel. The total field of view of the reducer was 6.1′ × 6.1′. The observations were carried out in the standard Johnson B and V bands. An exposure of twilight sky was used as a flat field.

A detailed log of observations is presented in Table 2. Observations of the NGC 524 group were performed on the night of 21/22 August, 2007, under photometric conditions with a seeing of about 2″. We took exposures of six 6° fields centered on the brightest galaxies of the group: NGC 524, NGC 502, NGC 509, NGC 516, NGC 518, and NGC 532. We used the central galaxy of the group, NGC 524, as a photometric standard; the HYPERLEDA database contains a good set of aperture photoelectric-photometry data for this galaxy reduced to the standard Johnson system.

3. STRUCTURE OF DISK GALAXIES OF THE NGC 524 GROUP

Figure 1 presents $B-V$ color maps of the six brightest disk galaxies of the group. The lenticular galaxies NGC 524 and NGC 502 are viewed nearly face-on, and color maps indicate very red nuclei, with

the colors becoming bluer outward in a monotonic, axially symmetric fashion—the classical color gradient in early-type galaxies, usually interpreted as a gradient of the metallicity of the stellar population. On the contrary, the lenticular galaxies NGC 509 and NGC 516 are viewed strictly edge-on. Unlike NGC 524 and NGC 502, their nuclei are bluer than the main bodies of the galaxies. Outside the nucleus, NGC 509 shows uniform red colors without an appreciable trend for bluer colors with radius, while NGC 516 shows a thin bluish disk embedded in a redder structure that can be characterized as a thick

Table 2. Photometric observations of galaxies of the NGC 524 group

NGC	Filter	Total exposure, s	Spatial resolution
502	B	540	2.3″
502	V	240	2.1
509	B	540	2.0
509	V	300	2.0
516	B	540	2.2
516	V	240	2.0
518	B	540	1.9
518	V	240	2.1
524	B	60	1.8
524	V	30	2.3
532	B	360	1.8
532	V	180	2.3

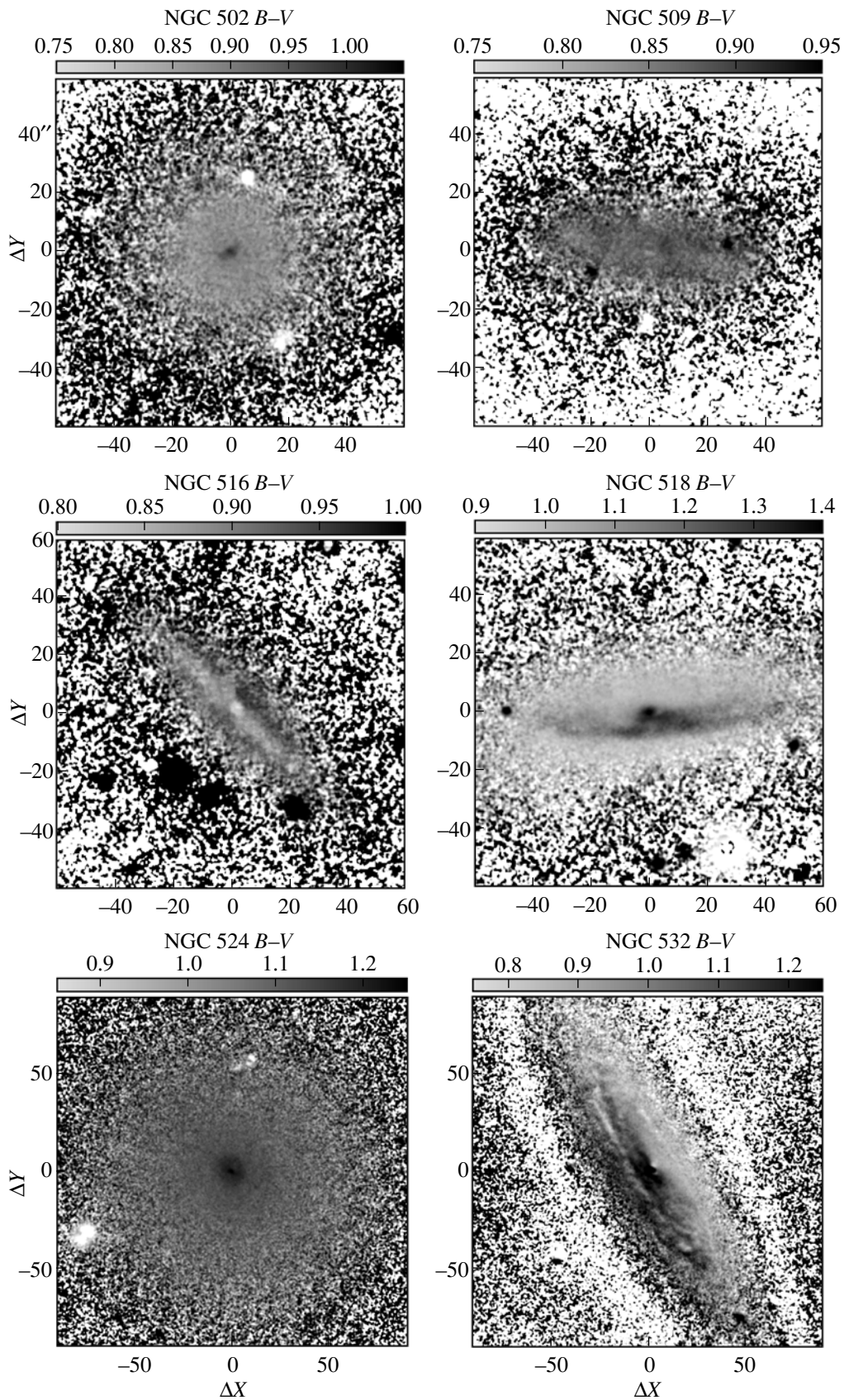


Fig. 1. $B-V$ color maps for the six large galaxies of the NGC 524 group.

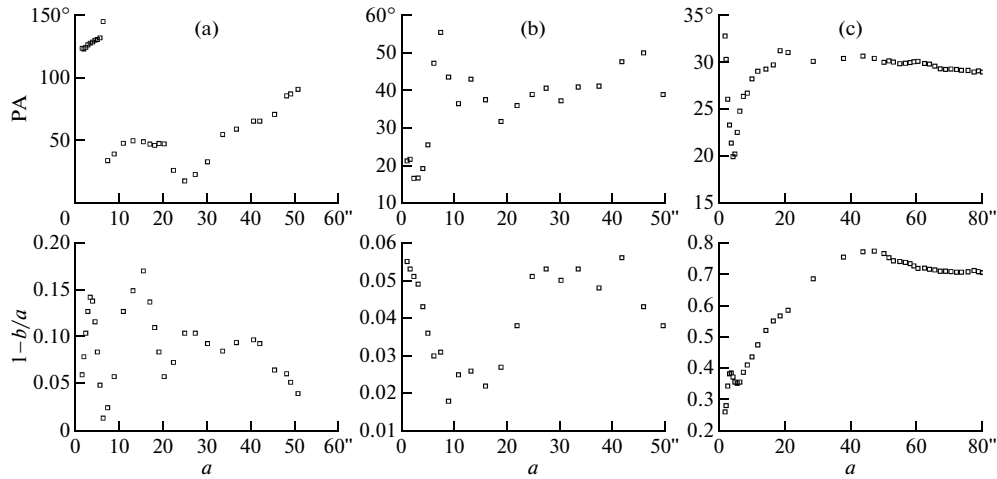


Fig. 2. Results of our isophotal analysis of the V images for (a) NGC 502, (b) NGC 524, and (c) NGC 532. The radial dependencies of the major-axis position angle (top) and the ellipticity of the isophotes (bottom) are shown.

disk. The color maps for the spiral galaxies NGC 518 and NGC 532 display strong dust lanes projected onto the bulges, which relate to the spiral arms of these galaxies; the displacement of the projections of the dust arms relative to the nucleus near the minor axis confirms our isophotal analysis, which suggests that these galaxies are not viewed strictly edge-on, but at an inclination of approximately 80° .

We performed an isophotal analysis and determined the major-axis position angles and ellipticities of the isophotes as a function of radius for all six galaxies in both filters. As a rule, the isophote ellipticity e reaches a plateau at some distance from the center and does not change further with radius. We assume that this level, $e \equiv 1 - b/a$, is related to the inclination of the galactic disk to the line of

sight i by the geometrical expression $\sqrt{\frac{2e - e^2}{1 - q_0^2}} =$

$\sin i$, where q_0 reflects the “thickness” of the disk and is equal to z_0/h . The corresponding radius represents the region where the thin outer stellar disk dominates the total surface brightness of the galaxy. In this region, we can determine the parameters of the exponential profile of the disk surface brightness [12] without including other structural components of the galaxy. A decomposition, i.e., a separation of the contributions of the spheroidal and disk components, is needed in more central regions. The behaviors of the isophote ellipticities in the central regions of NGC 524, NGC 502, and NGC 532 are more complex than is expected for the superposition of a spheroidal bulge and a flat disk. In NGC 524, the isophote ellipticity increases towards the center (Fig. 2b), NGC 532 has a local maximum of the ellipticity $4''$ from the center (Fig. 2c), and NGC 502

has two local ellipticity maxima at radii of $4''$ and $15''$ (Fig. 2a). The position angle also has a peculiar value near local maxima of the ellipticity: the major axis of the isophotes turns relative to the line of nodes of the galactic plane. This behavior of the isophotes suggests the presence of inner structures in the central regions of these galaxies, such as compact minibars, or tilted circumnuclear disks.

The large-scale structure of the galaxies was analyzed using the GIDRA [13] software, by using the obtained orientation parameters of the isophotes. The surface brightness profile was constructed by averaging over azimuth in elliptical rings, with a fixed center at the galactic center, and with the major axis and ellipticity corresponding to the isophotes at a given radius. The resulting profile was then successively decomposed into an exponential disk (or disks) and a Sersic bulge, starting from outer regions. This approach is not suitable for galaxies viewed edge-on, such as NGC 509 and NGC 516; for them, we made two linear cuts, along the major and minor axes, instead of averaging the surface brightness in rings. The cut along the minor axis was then used to estimate the bulge parameters, and the cut along the major axis was decomposed into the (already determined) bulge and second-order Bessel function(s) corresponding to the line-of-sight integral of the surface brightness of a round exponential disk that is optically thin up out to its edge. Table 3 presents the parameters of the resulting large-scale structural components.

Below we will comment on the derived structures of the individual galaxies.

NGC 502. The center of this galaxy has a very interesting structure: it seems at first that two bars with different sizes are embedded in each other (Fig. 2a).

Table 3. Parameters of photometric components of galaxies of the NGC 524 group

NGC	Filter	Outer disk			Inner disk			Bulge			
		μ_0 , mag/arcsec ²	r_0 , arcsec	r_0 , kpc	μ_0 , mag/arcsec ²	r_0 , arcsec	r_0 , kpc	n	μ_0 , mag/arcsec ²	r_0 , arcsec	r_0 , kpc
502	<i>B</i>	24.6	44.7	5.2	21.2	9.9	1.2	1.5	17.1	3.4	0.4
502	<i>V</i>	~23	39.3	4.6	20.1	10.5	1.2	1.5	15.8	3.53	0.4
509	<i>B</i>	20.6	33	3.8	—	—	—	1.5	17.4	3.0	0.35
509	<i>V</i>	19.6	33	3.8	—	—	—	1.5	16.2	2.8	0.3
516	<i>B</i>	23.0	24	2.8	19.8	11.5	1.3	1.8	17.9	3.0	0.35
516	<i>V</i>	21.9	29	3.4	18.5	13	1.5	1.9	16.6	2.84	0.3
518	<i>B</i>	22.9	34.4	4.0	21.2	16.4	2.0	2	17.1	8.2	0.95
518	<i>V</i>	21.6	35.4	4.1	19.8	16	1.9	2	16.4	6.67	0.8
524	<i>B</i>	21.5	30.9	3.6	19.5	9.0	1.05	1.2	17.9	3.1	0.4
524	<i>V</i>	20.3	30.9	3.6	18.3	8.6	1.0	1.2	16.6	2.8	0.3
532	<i>B</i>	20.8	70.2	8.2	19.45	18.7	2.2	2	17.0	6.0	0.7
532	<i>V</i>	20.45	73.2	8.5	18.2	20.5	2.4	2	15.7	4.8	0.55

We were able to trace the outer disk of the galaxy from a radius of $70''$, which has a very low surface brightness. A residual surface-brightness profile obtained after subtracting the first model disk has two “holes,” typical for a Freeman Type II profile. We fitted the profile using a second model disk in the interval from $23''$ to $60''$, assuming that there is a brightness excess, such as a ring, between $33''$ and $45''$. After subtracting the second model disk, the residual profile has a noticeable “hump” between $10''$ and $24''$. Based on the assumption that the model galaxy contains two exponential disks and a Sersic bulge, we fitted this profile with a somewhat flattened ($b/a = 0.91$) Sersic bulge with $n = 1.5$. The residual obtained by subtracting the three-component model from the initial image suggests that there is a nuclear bar with a radius of $6.5''$ and a ring located approximately between $5.9''$ and $20''$, with some brightness increase in the middle of this interval. Another possibility is that the central structure with a radius of $20''$ is a lens; but then there is no place for a bulge in this galaxy. Further analysis of kinematic data is needed to distinguish between these alternatives.

NGC 509. It appears that this galaxy is viewed edge-on, so that the GIDRA software cannot be used in this case. Unfortunately, a linear photometric cut can provide less information than a brightness profile averaged in rings (ellipses), due to the higher noise level, hindering “extension” of the profile to

large distances from the galactic center. It is probably for this reason that were distinguished only one exponential disk in the outer regions of this galaxy. The central regions of the profile, out to $9''$ from the nucleus, were fitted by a Sersic bulge with $n = 1.5$. The brightness profile has a clearly marked “hump,” or possibly a flat brightness profile, at radii from $9''$ to $44''$, as is typical of the lenses of S0 galaxies. A turn of the isophote position angle by 8° is visible in the radial dependences of the orientation parameters of the isophotes at radii of $7''$ – $30''$, and the isophote ellipticity shows a maximum (0.7); further, out to the edge of the outer disk, the isophote ellipticity drops to 0.4. This region ($7''$ – $30''$) has a uniformly red color. We can interpret this inner component as a lens. It may be that NGC 509 is not viewed quite edge-on, and that the turn of the isophotes indicates that the lens is non-axisymmetric. The galaxy apparently had structures such as a bar and ring, which have “dispersed” somewhat and spread over azimuth by the current moment.

NGC 516. This galaxy is viewed edge-on. Its surface brightness profile demonstrates a bend in the central region, as is typical for a Freeman Type II profile; this may indicate the presence of a bar in the galaxy. The maximum isophote ellipticity (0.7) is observed $20''$ from the center, supporting the hypothesis that a bar is present. The isophote ellipticity drops to 0.55 towards the galaxy’s edge. However, a thin, blue, edge-on disk “embedded” in a thicker

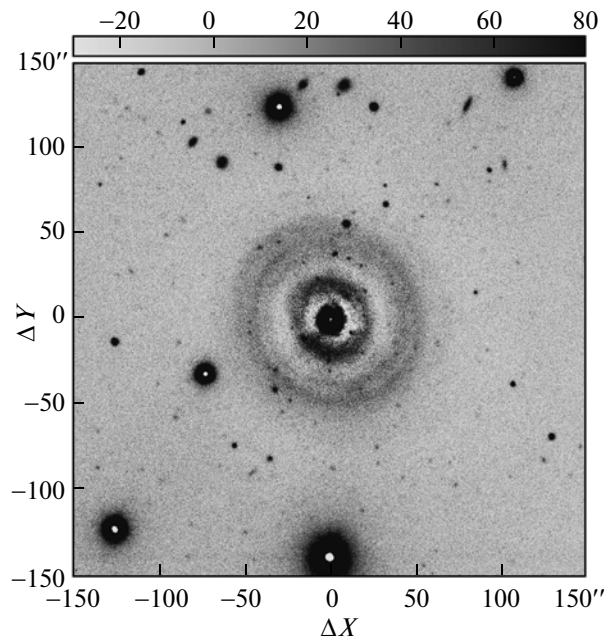


Fig. 3. Image of residual V brightness after subtraction of the total model for NGC 524 (two exponential disks and a Sersic bulge) from the initial image, showing rings with various radii in the surface-density distribution of the (old) stellar population.

reddish component is visible in the color map (Fig. 1), within about $25''$ of the center. It is possible that the excess brightness in this radius interval is due to the embedded young disk, and not a bar, which would not look uniformly blue along the whole of its length.

We modeled the disk component of the galaxy based on the approach described in [14, 15]. Note that the NGC 516 profile should be classified as a Type II profile. As a result, we distinguished outer and inner disks, as well as a bulge that dominates within $5''$ of the center.

NGC 518. According to the HYPERLEDA data, the galaxy's inclination to the line of sight is 82° . This is confirmed by the position of the galaxy's dust lane, which is clearly visible in the images and color map. Our isophotal analysis shows a constant isophote ellipticity (0.65) starting $35''$ from the center and extending to the disk edge. To obtain the surface-brightness profile, we constructed a photometric cut along the major axis of the object. A "hump" is visible in the profile between radii of $10''$ and $37''$, which is most likely the result of the intersection of our linear cut with the spiral pattern. We were able to fit the profile using two exponential disks and a Sersic bulge with $n = 2$.

NGC 524. The outer disk of this central galaxy of the group can be fitted with a model exponential disk starting from $70''$. The residual profile between $11''$ and $35''$ should be fitted with an inner disk. Rings extending to $R \approx 61''$ are clearly visible in the residual image. We continued the fitting using an almost

round Sersic bulge with a quasi-exponential profile ($n = 1.2$) within $11''$ from the galactic center. Subtracting the total model yields a residual containing a set of weak rings between $34''$ and $61''$, a bright ring at $R = 13''$ – $25''$, and, possibly, an inclined nuclear disk (Fig. 3).

Laurikainen et al. [16] recently performed a two-dimensional decomposition of an image NGC 524 in the K_s filter ($2 \mu\text{m}$ wavelength), which was less deep than the image analyzed by us here. They traced an outer exponential disk to a radius of $80''$ and noted the presence of two exponential segments with different scales in the residual profile within $R = 30''$. However, their model for the inner region consisted not of disks, but of a Sersic bulge with $n = 2.7$ and two "Ferrers" lenses with flat brightness profiles, which compensated the steep slope of the bulge brightness profile within radius intervals $R = 0''$ – $10''$ and $R = 10''$ – $30''$ each. It is obvious that, mathematically, the decomposition of the two-dimensional surface-brightness distribution into components admits more than one solution, especially if we do not restrict the number of components and their functional form. A final choice of the best model—bulge or disk—can be made only using kinematic data: stellar disks are dynamically cooler than spheroids, and their stellar velocity dispersions should be lower than those in bulges and lenses. We have already carried out a kinematic analysis of the stellar component of NGC 524 at various distances from the center, and

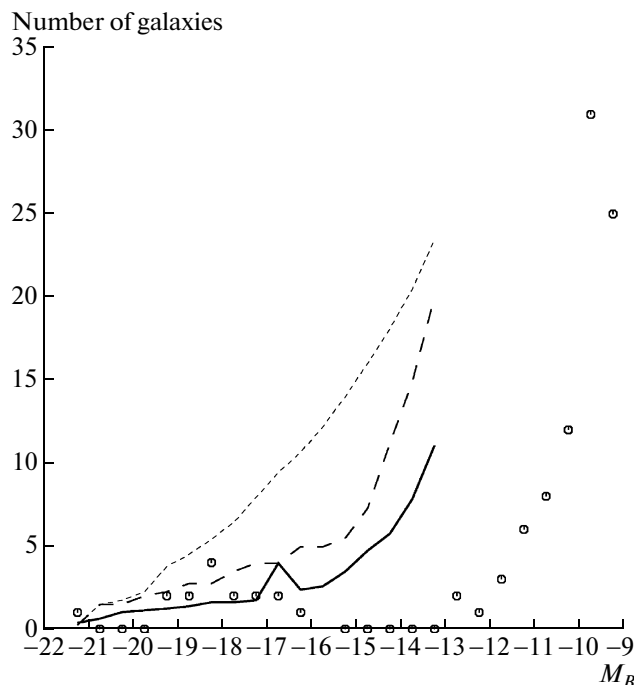


Fig. 4. Luminosity function of galaxies of the NGC 524 group in the interval $M_B = -22$ to -16 , according to the data of [3], and in the interval $M_B = -13$ to -9 , according to our measurements. For comparison, lines show the average luminosity functions of groups according to [20]: massive groups with high X-ray luminosities (dotted line), groups with intermediate masses and low X-ray luminosities (dashed line), and groups without X-ray emitting gas (solid line).

the kinematics indicate that the cool disk component dominates within $R = 10''$ – $30''$ [17].

NGC 532. The approximation of the outer parts of this galaxy with an exponential disk can start from $R = 125''$. The residual profile can be characterized as a Freeman Type II profile. We have fit this profile accurately using a model disk so as to retain the maximum information. After subtracting two exponential disks, spiral arms are clearly visible in the residual. Further modeling adds a small, strongly flattened bulge ($b/a = 0.68$) with Sersic parameter $n = 2$. It is difficult to see the circumnuclear structure due to the high inclination and dust content of the galaxy.

4. DWARF GALAXIES OF THE GROUP

In addition to our surface photometry of the largest members of the group, we also performed two-color aperture photometry of smaller galaxies within $6'$ fields around the main targets. We carried out photometry of all objects whose sizes exceeded the estimated full width at half maximum of stellar images. After forming a list of extended objects, $B-V$ color maps were made for each of them (Fig. 1) within a $3''$ – $4''$ aperture; since most of these galaxies are dwarfs (or compact remote objects), these colors can be considered to be the integral colors of the galaxies. The accuracy of the measured colors was estimated

from the spread of pixel values within the aperture used for the measurements (11×11 or 9×9 pixels), which ranges from 0.03^m for the brightest dwarfs to 0.2^m for the faintest. The $B-V$ color index was corrected for extinction in our Galaxy in accordance with [18]; $E(B-V) = 0.08$ was taken from the NED database. In all, 183 galaxies were measured in six fields.

Data of the SDSS-III survey covering a section of the sky containing the NGC 524 group became available through the Internet at the beginning of 2011; in particular, integrated $ugriz$ photometry (so-called “Petrosian” magnitudes) became available at the site <http://skyserver.sdss3.org/dr-8/en/tools/explore/>. Although the SDSS-III photometry is less deep than our own photometry (as we verified by comparing our $B-V$ color maps and the SDSS-III $g-r$ color maps for large galaxies of the group), we decided to use these data in order to distinguish background galaxies from dwarf members of the group. The photometric redshifts for galaxies having $ugriz$ magnitudes are calculated in the SDSS databases. The calculation of photometric redshifts is based on a so-called “learning sample”—a list of galaxies for which both photometry and spectroscopic redshifts are available. Unfortunately, the learning sample contains no dwarf spheroidal or dwarf irregular galaxies, for which very few spectra are available

Table 4. Coordinates, luminosities and colors of dwarf galaxies of the NGC 524 group

Number in the field	$\alpha_{2000.0}$	$\delta_{2000.0}$	M_B	$(B-V)_0$	Number in the field	$\alpha_{2000.0}$	$\delta_{2000.0}$	M_B	$(B-V)_0$
NGC 502 field					NGC 518 field				
1	01 ^h 23 ^m 04.3 ^s	+09°03'35"	-10.92	1.26	1	01 24 24.2	+09 20 58	-9.63	0.84
2	01 22 58.4	+09 04 39	-9.88	0.96	2	01 24 07.6	+09 21 06	-9.33	0.34
3	01 22 48.8	+09 04 02	-10.08	0.98	3	01 24 22.4	+09 18 27	-11.53	0.79
4	01 22 48.0	+09 03 49	-10.50	0.69	4	01 24 22.6	+09 17 17	-9.27	0.53
5	01 22 47.6	+09 02 09	-9.98	0.85	5	01 24 27.7	+09 18 27	-9.71	0.43
6	01 22 52.6	+09 00 25	-8.97	1.17	6	01 24 24.8	+09 17 08	-8.76	0.89
7	01 22 58.2	+09 01 39	-9.85	0.68	7	01 24 23.8	+09 17 30	-9.54	0.55
8	01 23 05.3	+09 00 49	-8.59	0.82	8	01 24 10.7	+09 22 01	-9.81	0.74
9	01 23 05.0	+09 00 58	-9.27	1.09	9	01 24 10.2	+09 21 52	-8.68	0.13
10	01 23 04.6	+09 00 47	-9.66	0.78	10	01 24 08.6	+09 20 02	-12.77	0.92
11	01 23 00.0	+09 00 37	-9.40	1.11	11	01 24 17.5	+09 21 21	-11.26	0.85
12	01 22 53.0	+09 03 25	-10.17	0.83	12	01 24 20.9	+09 22 22	-10.23	1.00
NGC 509 field					13	01 24 26.1	+09 17 53	-9.07	0.89
1	01 23 28.4	+09 28 01	-10.55	0.63	NGC 524 field				
2	01 23 27.3	+09 28 09	-8.93	0.32	1	01 24 52.4	+09 34 22	-10.46	1.14
3	01 23 27.9	+09 27 21	-9.55	0.98	2	01 24 49.7	+09 33 49	-11.31	1.29
4	01 23 23.4	+09 27 40	-11.52	0.93	3	01 24 54.3	+09 34 09	-10.23	0.06
5	01 23 13.1	+09 28 01	-9.87	0.32	4	01 24 53.0	+09 34 03	-12.02	0.98
6	01 23 16.9	+09 27 26	-8.81	0.36	5	01 24 51.9	+09 33 52	-12.71	1.05
7	01 23 20.3	+09 28 34	-9.53	0.60	6	01 24 42.4	+09 34 25	-11.57	1.16
8	01 23 19.8	+09 28 29	-8.69	0.55	7	01 24 41.0	+09 33 50	-11.22	0.50
9	01 23 20.8	+09 27 09	-9.03	0.34	8	01 24 45.6	+09 33 38	-10.48	0.77
10	01 23 23.7	+09 26 59	-9.05	0.48	9	01 24 53.6	+09 31 23	-10.38	0.78
11	01 23 19.8	+09 25 52	-10.35	0.95	10	01 24 50.7	+09 30 51	-10.51	0.84
12	01 23 14.2	+09 24 18	-9.90	0.44	11	01 24 44.7	+09 29 35	-10.50	0.82
13	01 23 24.1	+09 25 36	-10.21	0.63	12	01 24 44.1	+09 29 56	-9.94	0.10
14	01 23 24.4	+09 24 55	-10.28	0.70	NGC 532 field				
15	01 23 28.0	+09 24 19	-9.25	0.58	1	01 25 23.0	+09 16 51	-9.88	1.12
16	01 23 32.3	+09 27 18	-10.32	0.66	2	01 25 16.8	+09 18 28	-9.30	0.80
17	01 23 28.6	+09 27 42	-9.65	0.52	3	01 25 14.7	+09 18 34	-9.31	0.66
18	01 23 27.0	+09 27 33	-9.60	1.00	4	01 25 15.4	+09 18 01	-8.91	0.75
19	01 23 21.6	+09 26 42	-10.77	0.61	5	01 25 11.8	+09 16 52	-9.35	0.69
20	01 23 19.7	+09 27 45	-9.58	0.38	6	01 25 08.5	+09 15 19	-9.39	0.25
21	01 23 24.6	+09 27 01	-8.82	0.93	7	01 25 07.2	+09 15 17	-9.79	1.22
22	01 23 24.6	+09 26 50	-11.22	0.46	8	01 25 07.6	+09 15 02	-9.54	0.47
NGC 516 field					9	01 25 21.5	+09 13 24	-9.70	0.98
1	01 24 11.0	+09 35 20	-11.29	0.86	10	01 25 26.7	+09 13 22	-9.86	0.53
2	01 24 15.6	+09 34 57	-9.37	1.09	11	01 25 28.5	+09 13 29	-9.83	0.81
3	01 23 59.6	+09 35 20	-9.88	0.72	12	01 25 22.3	+09 13 03	-9.27	0.09
4	01 24 05.6	+09 31 52	-9.71	1.00	13	01 25 20.2	+09 14 37	-9.89	0.49
5	01 24 14.6	+09 30 23	-9.06	1.18	14	01 25 24.7	+09 15 01	-9.83	0.86
6	01 24 12.7	+09 30 24	-9.20	0.58	15	01 25 17.8	+09 14 28	-10.25	0.65
7	01 24 06.1	+09 30 27	-10.67	0.94	16	01 25 20.5	+09 13 44	-9.59	0.49
8	01 24 18.2	+09 32 25	-9.97	0.73	17	01 25 22.5	+09 13 43	-9.72	0.72
9	01 24 16.0	+09 32 19	-9.00	1.25	18	01 25 14.6	+09 18 16	-9.12	1.10
10	01 24 06.8	+09 32 34	-11.43	1.13	19	01 25 09.5	+09 18 08	-9.16	0.08
11	01 24 06.7	+09 32 32	-10.97	1.10	20	01 25 08.9	+09 14 04	-9.00	0.59
12	01 24 15.6	+09 32 51	-9.62	0.84	21	01 25 24.3	+09 13 34	-9.79	0.28
13	01 24 16.2	+09 33 01	-9.41	0.94	22	01 25 23.2	+09 13 25	-9.15	0.65
14	01 24 16.6	+09 33 08	-9.39	0.76	23	01 25 24.2	+09 14 10	-9.16	0.47
					24	01 25 24.1	+09 14 26	-9.29	0.14

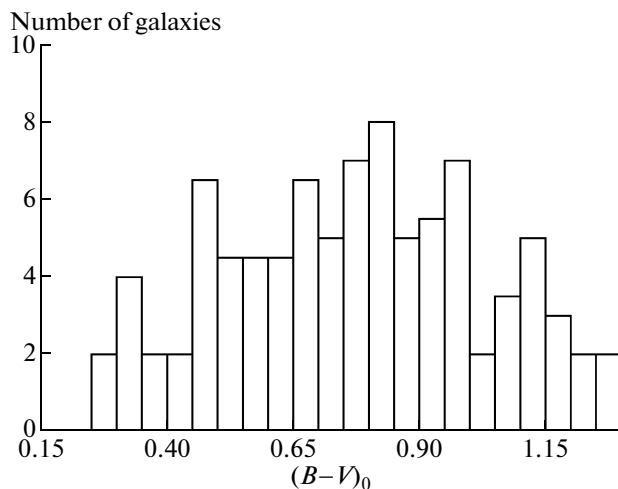


Fig. 5. Distribution of dwarf galaxies of the NGC 524 group according to their $B-V$ colors (corrected for the reddening in our Galaxy).

in the nearby Universe, severely hampering attempts to determine photometric redshifts for dwarf members of the NGC 524 group.

Based on the estimated typical accuracy of photometric redshifts in the SDSS survey, 0.035 [19], we rejected galaxies with measured SDSS photometric redshifts having accuracies better than 0.07 (2σ) from our list of candidate dwarf galaxies of the NGC 524 group. We then verified visually the morphology of the remaining candidates and required that the corrected $B-V$ color should be bluer than 1.3. As a result, 97 objects remained in the list of dwarf galaxies of the NGC 524 group, in the six fields analyzed, covering approximate radii of 30 kpc around large galaxies of the group. For most of these, we converted the integrated SDSS g magnitudes to absolute B magnitudes using the relationship between the $ugriz$ and $UBVRI$ photometric systems given by [20]; for galaxies without SDSS photometry, we measured the B magnitudes using our own data, taking fluxes in a series of increasing apertures until the background level was reached beyond the outermost aperture. We then corrected the B magnitudes for extinction in our Galaxy according to the recommendations of NED and converted these to absolute magnitudes using distance modulus to the group (31.9) [10]. Final results for the entire list of measured dwarf galaxies are given in Table 4.

It is interesting that our lists contain no galaxies brighter than $M_B = -13^m$, and such galaxies were also not found in wider neighborhoods of the studied fields, which we scanned using a navigator of the eighth SDSS data release. Since the NED database likewise does not find any such galaxies during a search for members of the group over the total area of the group, we conclude that there are no group

galaxies with absolute magnitudes between $M_B = -13^m$ and -16^m , i.e., the luminosity function of the group members is clearly bimodal.

Figure 4 presents the luminosity function of the identified dwarfs and of the 16 large members of the group, for which we took the integrated blue magnitudes from [3]. Generally speaking, we must match the two parts of the luminosity function—for large and small galaxies, with a boundary near $M_B = -16$ —by multiplying the dwarf branch by a factor related to the fact that we have not studied the full area of the group. Assuming a uniform distribution of dwarf galaxies over the group area, this factor should be 35. However, Fig. 4 shows that so substantial correction is not needed, and the required factor does not exceed 10: apparently, the dwarfs are concentrated toward the large galaxies, being satellites of the latter.

Figure 4 also compares the luminosity function of the members of the NGC 524 group with the average luminosity functions of various mass groups given in [21]. The slope of the dwarf branch is consistent with all the average luminosity functions (although it is shifted by several magnitudes to the region of weak galaxies). In the bright part of the luminosity function, the number of galaxies in the NGC 524 group agrees with the luminosity functions of groups with zero or low X-ray luminosities (with low or intermediate total masses), and a bimodal luminosity function is generally a sign of groups without X-ray emitting gas [21]. The ROSAT data give an X-ray luminosity of $\log L_X [\text{erg/s}] = 41.05$ for the NGC 524 group [7], but there is a note that the X-ray emission is concentrated in the halo of the central galaxy, NGC 524. Thus, the shape of the luminosity function for galaxies in the NGC 524 group supports the idea that group *does not have* hot intergalactic gas.

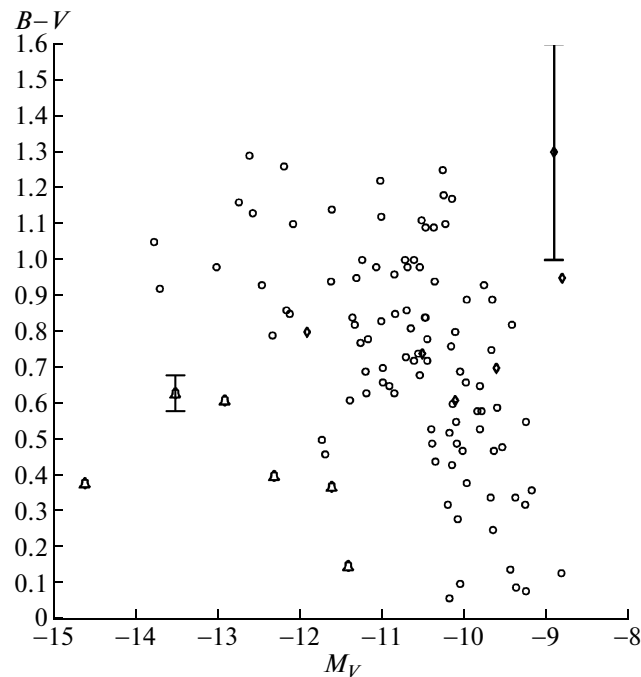


Fig. 6. Color–luminosity diagram for dwarf galaxies of the NGC 524 group compared to dwarf galaxies of the Local Group. The circles show dwarf galaxies of the NGC 524 group, the bells late-type dwarfs of the Local Group with young stellar populations, and the diamonds dSph dwarfs of the Local Group with old stellar populations.

Figure 5 presents the $B-V$ color distribution for the dwarf galaxies. This distribution is approximately flat in the color interval $B-V = 0.4-1.0$: we do not see the usual bimodality, with a “red sequence” and “blue cloud.” Initially we could suppose, based on the example of our Local Group, that red dwarfs are concentrated near large “parent galaxies” and blue dwarfs are located far from such galaxies, because tidal effects from large galaxies suppress star formation in their satellites. However, in our case, a considerable number of blue dwarfs with star formation were found near large galaxies.

The color–luminosity diagram in Fig. 6 compares the dwarf populations of the NGC 524 group and the Local Group (data for the Local Group were taken from [22]). Dwarfs of both early (dSph) and late (dIrr) types were selected over the Local Group for completeness, and are presented in the color–luminosity diagram together with members of the NGC 524 group. The dwarfs of the Local Group and NGC 524 group occupy approximately the same color interval; the reddest dwarf of the Local Group, Ursa Minor, is a dSph dwarf with $B-V = 1.3 \pm 0.3$, like the reddest dwarfs of the NGC 524 group. However, the bluest dwarfs of the Local Group are more luminous than the bluest dwarfs located near large galaxies of the NGC 524 group, on average by approximately 2^m .

5. CONCLUSION

We have analyzed the structures of the six largest disk galaxies of the NGC 524 group using surface photometry obtained at the SAO 6-m telescope with the SCORPIO reducer. Four of these are classified in the literature as lenticular galaxies, and another two are classified as early-type spiral galaxies; two galaxies are viewed almost face-on, while the remaining four are inclined at large angles to the line of sight. As far as we can judge from their images, none of the galaxies viewed *not quite* edge-on has a large-scale bar. Based on the behavior of the radial surface-brightness distribution, the only galaxy that may contain a bar is NGC 516, which is viewed strictly edge-on; though it may be not a bar, but instead an embedded, thin inner edge-on disk. In general, bars are present in 40–70% of disk galaxies; their absence in all the large galaxies of the NGC 524 group could indicate some influence from their environment.

However, we detected both inner and rather large rings in almost all the large disk galaxies in the NGC 524 group. In the face-on galaxies NGC 502 and NGC 524, rings of different radii fill almost the entire range of distances from the center in the optical disks. The statistics of the presence of bars in disk galaxies indicates that about 50% of such galaxies have inner rings [23], while 20% have nuclear rings (with radii out to 1.5 kpc) [24], with a bar being present in the overwhelming majority of galaxies with

rings. The disk galaxies of the NGC 524 group have rings but no bars. It is interesting that no neutral hydrogen was found in the four lenticular galaxies of the group [9]; i.e., there is no gas and so no star formation, but there are rings (waves) of surface brightness. If such structural anomalies are to be explained by an enhanced contribution of secular evolution during the formation of the large-scale structure of the galaxies in a dense environment, we must identify mechanisms that do not switch on star formation, for which there is no fuel in this case. Here we must also explain why the Sersic exponents of the bulges of all the group members are only two or even lower: bulges built via the secular evolution of disks with bars and gas have exponential bulges, while “minor merging” (the capture of satellites) usually increases the Sersic exponents in bulges to 3–4 [25].

The presence of a large number of blue dwarf galaxies undergoing ongoing star formation within 20–30 kiloparsec from large galaxies of the group is interesting. Dynamical evolution over scales of a few billion years should cause these dwarfs to “fall” into their parent galaxies, or at least deprive them of gas and ongoing star formation, as in the Local Group. Thus, systems of blue dwarfs around large red galaxies should either be very young systems, or be in stable orbits that prevent their falling into their parent galaxies; otherwise, the continuous accretion of gas-rich dwarfs onto the disks of lenticular galaxies would provide large galaxies with fuel for ongoing star formation. This does not occur for some reason: our spectral studies have shown that the outer disks of NGC 502 and NGC 524 have very old stellar populations [26].

ACKNOWLEDGMENTS

The data used in this study were obtained at the 6-m telescope of the Special Astrophysical Observatory of the Russian Academy of Sciences, operated with financial support from the Ministry of Education and Science of the Russian Federation (registration number 01-43). We thank A.V. Moiseev for support of these observations. The data analysis made use of the Lyon–Meudon Extragalactic Database (LEDA), maintained by the LEDA team at the Lyon Centre for Astrophysics Research (CRAL; France), and the NASA/IPAC Extragalactic Database (NED), operated by the Jet Propulsion Laboratory of the California Institute of Technology under contract with the National Aeronautics and Space Administration (USA). We also used public data of the SDSS-III project (<http://www.sdss3.org>), supported by the Alfred P. Sloan Foundation, the participating institutions of the SDSS Collaboration, the National Science Foundation, and the U.S. Department of Energy Office of Science. This work was supported by the

Russian Foundation for Basic Research (project 10-02-00062a).

REFERENCES

1. J. Kormendy and R. C. Kennicutt, Jr., *Ann. Rev. Astron. Astrophys.* **42**, 603 (2004).
2. M. J. Geller and J. P. Huchra, *Astrophys. J. Suppl. Ser.* **52**, 61 (1983).
3. J. Vennik, *Baltic Astron.* **1**, 415 (1992).
4. S. Brough, D. A. Forbes, V. A. Kilborn, and W. Couch, *Mon. Not. R. Astron. Soc.* **370**, 1223 (2006).
5. D. Makarov and I. Karachentsev, *Mon. Not. R. Astron. Soc.* **412**, 2498 (2011).
6. D. A. Forbes, T. Ponman, F. Pearce, et al., *Publ. Astron. Soc. Austral.* **23**, 38 (2006).
7. J. Osmond and T. Ponman, *Mon. Not. R. Astron. Soc.* **350**, 1511 (2004).
8. G. de Vaucouleurs, A. de Vaucouleurs, H. G. Corwin, Jr., et al., *Third Reference Catalogue of Bright Galaxies. Volume I: Explanations and References* (Springer, New York, 1991).
9. Ch. Sengupta and R. Balasubramanyam, *Mon. Not. R. Astron. Soc.* **369**, 360 (2006).
10. J. L. Tonry, A. Dressler, J. P. Blakeslee, et al., *Astrophys. J.* **546**, 681 (2001).
11. V. L. Afanasiev and A. V. Moiseev, *Astron. Lett.* **31**, 194 (2005).
12. K. C. Freeman, *Astrophys. J.* **160**, 767 (1970).
13. A. V. Moiseev, J. R. Valdés, and V. H. Chavushyan, *Astron. Astrophys.* **421**, 433 (2004).
14. P. Erwin, M. Pohlen, and J. E. Beckman, *Astron. J.* **135**, 20 (2008).
15. L. Gutiérrez, P. Erwin, R. Aladro, and J. E. Beckman, *Astron. J.* **142**, 145 (2011).
16. E. Laurikainen, H. Salo, R. Buta, and J. H. Knapen, *Astrophys. J.* **692**, L34 (2009).
17. I. Katkov, I. Chilingarian, O. Sil'chenko, et al., *Baltic Astron.* **20**, 453 (2011).
18. D. J. Schlegel, D. P. Finkbeiner, and M. Davis, *Astrophys. J.* **500**, 525 (1998).
19. D. Sowards-Emmerd, J. A. Smith, T. A. McKay, et al., *Astron. J.* **119**, 2598 (2000).
20. T. S. Chonis and C. M. Gaskell, *Astron. J.* **135**, 264 (2008).
21. T. A. Miles, S. Raychaudhury, D. A. Forbes, et al., *Mon. Not. R. Astron. Soc.* **355**, 785 (2004).
22. M. L. Mateo, *Ann. Rev. Astron. Astrophys.* **36**, 435 (1998).
23. R. Buta and F. Combes, *Fundam. Cosmic Phys.* **17**, 95 (1996).
24. S. Comerón, J. H. Knapen, J. E. Beckman, et al., *Mon. Not. R. Astron. Soc.* **402**, 2462 (2010).
25. J. A. L. Aguerri, M. Balcells, and R. F. Peletier, *Astron. Astrophys.* **367**, 428 (2001).
26. O. K. Sil'chenko, I. S. Proshina, A. P. Shulga, and S. E. Kuposov, *Mon. Not. R. Astron. Soc.* (2012, in press).

Translated by O. Merkulova